

**DEVELOPMENT OF AN IMMUNOASSAY FOR
MITRAGYNINE**

LEE MEI JIN

UNIVERSITI SAINS MALAYSIA

2016

**DEVELOPMENT OF AN IMMUNOASSAY FOR
MITRAGYNINE**

by

LEE MEI JIN

**Thesis submitted in fulfillment of the requirements
for the Degree of
Doctor of Philosophy**

May 2016

ACKNOWLEDGEMENT

First, I would like to thank my helpful supervisor, Professor Dr. Tan Soo Choon, who guides me in completing my research project. The supervision and support that he gave truly helped and boosted my progress in the research. Besides, I want to thank my co-supervisor, Professor Dr. Surash Ramanathan and Professor Dr. Sharif Mahsufi Mansor from Centre of Drug Research (CDR). They provided me mitragynine which had been extracted from the plant of kratom and human urine samples from kratom users. Much appreciated go to my institute - Institute for Research in Molecular Medicine (INFORMM, Penang) for giving me permission to commence this research. My grateful thanks go to the MyBrain15 that provides me MyPhD scholarship and HiCOE grant which funded this project. I also wish to thank Veterinary Research Institute (VRI), Ipoh for assisting me to carry out the animal work at the VRI. Also my deepest gratitude to Mr. Ramlee bin Abdul Wahab from glass blowing workshop, school of chemical sciences in University Sains Malaysia, Penang. The co-operation was much indeed appreciated. Not forgetting my family who encouraged me throughout my journey in completing the research. Last but not least, I would like to thank Usains Biomics Laboratory Testing Services SDN. BHD. and my lab mates and friends who work together. Special thanks to Miss Ang Chee Wei, Mr. Sim Hann Liang, Dr. Chan Sue Hay and Dr. Ashraf Ali Mohamed Kassim for all the advices and ideas throughout the project.

TABLE OF CONTENTS

	Page
ACKNOWLEDGEMENT	ii
TABLE OF CONTENTS	iii
LIST OF TABLES	xvi
LIST OF FIGURES	xxi
LIST OF ABBREVIATIONS	xxix
LIST OF SYMBOLS	xxxiv
ABSTRAK	xxxv
ABSTRACT	xxxvii
CHAPTER 1 – INTRODUCTION	1
1.1 <i>Mitragyna speciosa</i>	1
1.2 Chemical constituents of <i>Mitragyna speciosa</i>	4
1.2.1 Mitragynine	11
1.2.2 7 α -Hydroxy-7H-mitragynine	13
1.3 Abuse of kratom	13
1.4 Problem statement	16
1.5 Objectives of study	18
CHAPTER 2 – HAPTEN MODIFICATION AND CONJUGATION	19
2.1 Introduction	19
2.2 Aim of study	24

2.3	Materials and instrumentation	24
2.4	Methods	29
2.4.1	Modification of hapten mitragynine	29
2.4.1(a)	Synthesis of 4-aminobenzoic acid-mitragynine (PABA-MG) via diazotization of mitragynine	29
2.4.1(b)	Synthesis of 9-hydroxymitragynine (9-O-DM-MG) via demethylation of mitragynine	32
	i) Demethylation of mitragynine using ethanethiol	32
	ii) Demethylation of mitragynine using dimethyl sulfide	34
	iii) Demethylation of mitragynine using iodocyclohexane	34
2.4.1(c)	Synthesis of 16-carboxymitragynine (16-COOH-MG) via hydrolysis of mitragynine	35
	i) Hydrolysis of mitragynine using trimethyltin hydroxide	35
	ii) Acid hydrolysis of mitragynine using methanolic HCl	36
	iii) Alkaline hydrolysis of mitragynine using sodium hydroxide	37
	iv) Alkaline hydrolysis of mitragynine using potassium hydroxide	37
	v) Alkaline hydrolysis of mitragynine using lithium hydroxide	39
2.4.1(d)	Alkylation of mitragynine	39
	i) Alkylation of mitragynine using ethyl-5-bromovalerate	39

	ii)	Alkylation of mitragynine using 3-bromopropionic acid (cold condition)	42
	iii)	Alkylation of mitragynine using 3-bromopropionic acid (hot condition)	43
	iv)	Alkylation of mitragynine using 3-iodopropionic acid	43
2.4.1(e)		Reduction of mitragynine	44
	i)	Reduction of mitragynine using sodium borohydride	44
	ii)	Reduction of mitragynine using lithium aluminium hydride	45
2.4.1(f)		Oxidation of mitragynine using potassium permanganate	46
2.4.2		Conjugation of hapten to carrier protein	46
2.4.2(a)		Conjugation of mitragynine via Mannich reaction	46
	i)	Synthesis of cationized-bovine serum albumin (cBSA)	46
	ii)	Synthesis of MG-cBSA	47
	iii)	Synthesis of BSA-6-aminocaproic acid (BSA-6-ACA)	47
	iv)	Synthesis of MG-BSA-6-ACA	48
	v)	Synthesis of BSA-bis-(3-aminopropyl-amine) (BSA-bis-(3-APA))	49
	vi)	Synthesis of MG-BSA-bis-(3-APA)	49
	vii)	Synthesis of MG-KLH	50
	viii)	Synthesis of MG-multiple antigen peptides-16 (MG-MAPs-16)	51

2.4.2(b)	Conjugation of PABA-MG via carbodiimide method	52
	i) Synthesis of PABA-MG-BSA	52
	ii) Synthesis of PABA-MG-cBSA	52
	iii) Synthesis of PABA-MG-KLH	53
2.4.2(c)	Conjugation of 9-O-DM-MG via homobifunctional linker (BDDE)	54
	i) Synthesis of 9-O-DM-MG-BSA	54
	ii) Synthesis of 9-O-DM-MG-KLH	54
2.4.2(d)	Conjugation of 16-COOH-MG via carbodiimide method	56
	i) Synthesis of 16-COOH-MG-BSA	56
	ii) Synthesis of 16-COOH-MG-KLH	56
2.4.2(e)	Synthesis of MG-BSA via photoactivation using Sulfo-NHS-SS-Diazirine (sulfo-SDAD)	57
2.4.3	Conjugation of enzyme tracers	59
2.4.3(a)	Conjugation of horseradish peroxidase (HRP) to mitragynine via Mannich reaction	59
2.4.3(b)	Conjugation of HRP to PABA-MG via carbodiimide method	59
2.4.3(c)	Conjugation of HRP to 9-O-DM-MG via homobifunctional linker (BDDE)	60
2.4.3(d)	Conjugation of HRP to 16-COOH-MG via carbodiimide method	61
2.4.4	Determination of protein-hapten conjugates concentration	62
2.4.5	Determination of coupling efficiency of protein-hapten conjugates	63

	2.4.5(a)	2,4,6-trinitrobenzene sulfonic acid (TNBS) assay	63
	2.4.5(b)	Matrix-Assisted Laser Desorption Ionization-Time of Flight (MALDI-TOF) mass spectrometry	64
2.5		Results and discussion	64
	2.5.1	Modification of hapten mitragynine	64
	2.5.1(a)	Synthesis of 4-aminobenzoic acid-mitragynine (PABA-MG) via diazotization of mitragynine	64
	2.5.1(b)	Synthesis of 9-hydroxymitragynine (9-O-DM-MG) via demethylation of mitragynine	66
	2.5.1(c)	Synthesis of 16-carboxymitragynine (16-COOH-MG) via hydrolysis of mitragynine	72
	2.5.1(d)	Alkylation of mitragynine	74
	2.5.1(e)	Reduction of mitragynine	75
	2.5.1(f)	Oxidation of mitragynine	76
	2.5.2	Conjugation of hapten to carrier protein	76
	2.5.2(a)	Synthesis of MG-cBSA, MG-BSA-6-ACA, MG-BSA-bis-(3-APA), MG-KLH, and MG-MAPs-16 via Mannich reaction	76
	2.5.2(b)	Conjugation of PABA-MG to BSA, cBSA, and KLH via carbodiimide method	79
	2.5.2(c)	Conjugation of 9-O-DM-MG to BSA and KLH via BDDE linker	81
	2.5.2(d)	Conjugation of 16-COOH-MG to BSA and KLH via carbodiimide method	81
	2.5.2(e)	Synthesis of MG-BSA via photoactivation using Sulfo-NHS-SS-Diazirine (sulfo-SDAD)	81
	2.5.3	Conjugation of enzyme tracers	82

2.5.4	Determination of protein-hapten conjugates concentration	82
2.5.5	Determination of coupling efficiency of protein-hapten conjugates	89
2.5.5(a)	2,4,6-trinitrobenzene sulfonic acid (TNBS) assay	89
2.5.5(b)	Matrix-Assisted Laser Desorption Ionization-Time of Flight (MALDI-TOF) mass spectrometry	91
2.6	Conclusion	94
 CHAPTER 3 – IMMUNIZATION AND ANTIBODIES ASSESSMENT		96
3.1	Introduction	96
3.2	Aim of study	104
3.3	Materials and instrumentation	104
3.4	Methods	106
3.4.1	Preparation of immunogen and immunization schedule	106
3.4.2	Antibody harvesting	107
3.4.3	Antibody purification	108
3.4.4	Preparation of immunoassay reagents	108
3.4.4(a)	Preparation of wash buffer (10 times concentrate)	108
3.4.4(b)	Preparation of 0.1 M phosphate buffered saline (PBS)	109
3.4.4(c)	Preparation of 0.01 M phosphate buffered saline (PBS)	109
3.4.4(d)	Preparation of dilution buffer/antibody binding buffer	109

3.4.4(e)	Preparation of coating buffer	109
3.4.4(f)	Preparation of stabilizer solution	109
3.4.4(g)	Preparation of 2 N hydrochloric acid (HCl) solution	110
3.4.4(h)	Preparation of saturated ammonium sulphate solution	110
3.4.5	Protocol on plate coating	110
3.4.5(a)	Coating of protein A-Sheep-Anti-Rabbit (PASAR) antibody plate	110
3.4.5(b)	Coating of protein A-Sheep-Anti-Mouse (PASAM) antibody plate	111
3.4.6	Rabbit Anti-mitragynine antibody titre assessment	111
3.4.7	Mouse Anti-mitragynine antibody titre assessment	112
3.5	Results and discussion	113
3.6	Conclusion	119
CHAPTER 4 – DEVELOPMENT OF AN ENZYME-LINKED IMMUNOSORBENT ASSAY AGAINST MITRAGYNINE & ITS METABOLITES AND ASSAY OPTIMIZATION & VALIDATION		120
4.1	Introduction	120
4.2	Aim of study	130
4.3	Materials and instrumentation	131
4.4	Methods	133
4.4.1	Direct competitive enzyme immunoassay standard protocol	133
4.4.2	Optimization of ELISA assay using antibody from immunogen PABA-MG-BSA	134
4.4.2(a)	Determination of optimum dilution of enzyme-conjugate and antibody	134

	4.4.2(b)	Determination of half maximal inhibitory concentration (IC ₅₀)	135
4.4.3		Optimization of ELISA assay using antibody from immunogen MG-cBSA	135
	4.4.3(a)	Determination of ELISA assay performance using enzyme-conjugates, HRP-MG and HRP-PABA-MG	135
	4.4.3(b)	Determination of optimum dilution of enzyme-conjugate (HRP-MG) and antibody (from immunogen MG-cBSA) in dilution buffer	136
	4.4.3(c)	Linear range of calibration curve using enzyme-conjugate and antibody in dilution buffer	137
	4.4.3(d)	Antibody cross-reactivity study using enzyme-conjugate HRP-MG	138
	4.4.3(e)	Reduction of matrix effects	138
	4.4.3(f)	Stability study of enzyme-conjugate (HRP-MG)	139
	4.4.3(g)	Stability study of antibody from immunogen MG-cBSA	139
	4.4.3(h)	Stability study of calibrators of mitragynine	139
	4.4.3(i)	Linear range of calibration curve using enzyme-conjugate and antibody in stabilizer (HRP Stabilzyme)	140
	4.4.3(j)	Determination of ELISA assay sensitivity	140
4.4.4		Method validation for ELISA assay	141
	4.4.4(a)	Intra-day assay (Precision)	141
	4.4.4(b)	Inter-day assay (Reproducibility)	141
4.4.5		Assay of urine samples collected from kratom users	141
4.5		Results and discussion	142

4.5.1	Optimization of ELISA assay using antibody from immunogen PABA-MG-BSA	143
4.5.1(a)	Determination of optimum dilution of enzyme-conjugate and antibody	143
4.5.1(b)	Determination of half maximal inhibitory concentration (IC ₅₀)	145
4.5.2	Optimization of ELISA assay using antibody from immunogen MG-cBSA	147
4.5.2(a)	Using HRP-MG (Mannich reaction)	147
4.5.2(b)	Using HRP-PABA-MG	147
4.5.2(c)	Determination of optimum dilution of enzyme-conjugate (HRP-MG) and antibody (from immunogen MG-cBSA) in dilution buffer	148
4.5.2(d)	Linear range of calibration curve using enzyme-conjugate and antibody in dilution buffer	149
4.5.2(e)	Antibody cross-reactivity study using enzyme-conjugate HRP-MG	150
4.5.2(f)	Reduction of matrix effects	152
4.5.2(g)	Stability study of enzyme-conjugate (HRP-MG)	153
4.5.2(h)	Stability study of antibody from immunogen MG-cBSA	156
4.5.2(i)	Stability study of calibrators of mitragynine	158
4.5.2(j)	Linear range of calibration curve using enzyme-conjugate and antibody in stabilizer (HRP Stabilzyme)	160
4.5.2(k)	Determination of ELISA assay sensitivity	161
4.5.3	Method validation for ELISA assay	163
4.5.3(a)	Intra-day assay (Precision)	163

4.5.3(b)	Inter-day assay (Reproducibility)	165
4.5.4	Assay of urine samples collected from kratom users	166
4.6	Conclusion	167
CHAPTER 5 – DEVELOPMENT AND VALIDATION OF LIQUID CHROMATOGRAPHY TANDEM MASS SPECTROMETRY METHOD FOR THE DETECTION OF MITRAGYNINE AND ITS METABOLITES IN HUMAN URINE SAMPLES		170
5.1	Introduction	170
5.2	Aim of study	175
5.3	Materials and instrumentation	175
5.4	Methods	177
5.4.1	LC-MS/MS fragmentation of mitragynine and internal standard	177
5.4.2	Urine extraction for mitragynine and its metabolites	177
	5.4.2(a) Urine extraction without hydrolysis	177
	5.4.2(b) Urine extraction with hydrolysis	178
5.4.3	Development of MRM method	179
5.4.4	Standard calibration curves for mitragynine, 9-hydroxymitragynine (9-O-DM-MG), and 16-carboxymitragynine (16-COOH-MG)	180
5.4.5	Method validation	181
	5.4.5(a) Selectivity of the LC-MS/MS method	181
	5.4.5(b) Intra-day assay reproducibility	181
	5.4.5(c) Inter-day assay reproducibility	182
	5.4.5(d) Limit of quantification (LoQ)	182
5.4.6	Quantification of positive urine for mitragynine, 9-O-DM-MG, and 16-COOH-MG	183

5.4.7	Determination of phase II metabolites in positive human urine	184
	5.4.7(a) Glucuronide conjugates	184
	5.4.7(b) Sulphate conjugates	184
5.4.8	Determination of the degree of hydrolysis of sulphate metabolites by enzyme β -glucuronidase/arylsulfatase from <i>Helix pomatia</i>	185
5.4.9	Isolation of 9- <i>o</i> -demethyl MG sulphate (9-O-DM-S-MG), 9- <i>o</i> -demethyl MG glucuronide (9-O-DM-G-MG), 16-carboxy MG glucuronide (16-COOH-G-MG), 17- <i>o</i> -demethyl-16,17-dihydro MG glucuronide (17-O-DM-DH-G-MG), 9- <i>o</i> -demethyl-16-carboxy MG sulphate (9-O-DM-16-COOH-S-MG) metabolites from positive human urine	185
5.4.10	Cross-reactivity of the 9-O-DM-G-MG, 9-O-DM-S-MG, 16-COOH-G-MG, 9-O-DM-16-COOH-S-MG, and 17-O-DM-DH-G-MG metabolites isolated from human urine	187
5.4.11	Correlation study between LC-ESI-MS/MS and ELISA	187
5.5	Results and discussion	187
5.5.1	LC-MS/MS fragmentation of mitragynine and internal standard	187
5.5.2	Urine extraction for mitragynine and its metabolites	189
5.5.3	Development of MRM method	191
5.5.4	Standard calibration curves for mitragynine, 9-O-DM-MG, and 16-COOH-MG	194
5.5.5	Method validation	197
	5.5.5(a) Selectivity of the LC-MS/MS method	197
	5.5.5(b) Intra-day and inter-day assay reproducibility	202
	5.5.5(c) Limit of quantification (LoQ)	204
5.5.6	Quantification of positive urine for mitragynine, 9-O-DM-MG, and 16-COOH-MG	206

5.5.7	Determination of phase II metabolites in positive human urine	207
5.5.8	Determination of the degree of hydrolysis of sulphate metabolites by enzyme β -glucuronidase/arylsulfatase from <i>Helix pomatia</i>	208
5.5.9	Isolation of 9-O-DM-S-MG, 9-O-DM-G-MG, 16-COOH-G-MG, 17-O-DM-DH-G-MG, 9-O-DM-16-COOH-S-MG metabolites from the positive human urine	209
5.5.10	Cross-reactivity of the 9-O-DM-G-MG, 9-O-DM-S-MG, 16-COOH-G-MG, 9-O-DM-16-COOH-S-MG, and 17-O-DM-DH-G-MG metabolites isolated from human urine	210
5.5.11	Correlation study between LC-ESI-MS/MS and ELISA	211
5.6	Conclusion	215
CHAPTER 6 – GENERAL DISCUSSION AND CONCLUSION		217
6.1	General discussion	217
6.2	Conclusion	223
6.3	Future study	224
REFERENCES		225
APPENDICES		237
Appendix A	MALDI-TOF mass spectra for the synthesized hapten protein conjugates	237
Appendix B	Cross-reactivity data and stability data of ELISA	255
Appendix C	Certificate of ethical clearance	267
Appendix D	Animal ethics approval	278

Appendix E	Certificate of analysis	280
Appendix F	Characterization of mitragynine and its metabolites	290
LIST OF PUBLICATIONS		295

LIST OF TABLES

		Page
Table 1.1	Table showing the alkaloids found in <i>Mitragyna speciosa</i> .	6
Table 2.1	A comparison of conjugation ratio of hapten:carrier protein determined using the reference from TNBS assay and MALDI-TOF mass spectrometry method. N.A. refers to not applicable.	93
Table 2.2	Antigens that were successfully synthesized using the four methods that have been discussed in section 2.4.1 and 2.4.2. These antigens were used to immunize animal hosts in attempts to raise mitragynine antibodies.	95
Table 3.1	Comparison of rabbit anti-mitragynine antibodies (1 st – 9 th bleed) raised against PABA-MG-BSA in rabbit I and rabbit II. The antibodies were evaluated in terms of antibody response and affinity in a direct competitive ELISA.	114
Table 3.2	Comparison of rabbit anti-mitragynine antibodies (2 nd – 8 th bleed) raised against MG-cBSA in rabbit III and rabbit IV. The antibodies were evaluated in terms of antibody response and affinity in a direct competitive ELISA.	115
Table 3.3	Comparison of rabbit anti-mitragynine antibodies (1 st – 7 th bleed) raised against MG-BSA-6-ACA in rabbit V. The antibodies were evaluated in terms of antibody response and affinity in a direct competitive ELISA.	116
Table 3.4	Comparison of rabbit anti-mitragynine antibodies (3 rd – 5 th bleed) raised against 9-O-DM-MG-BSA in rabbit VI and rabbit VII. The antibodies were evaluated in terms of antibody response and affinity in a direct competitive ELISA.	116
Table 3.5	Comparison of rabbit anti-mitragynine antibodies (1 st bleed – 3 rd bleed) raised against 16-COOH-MG-BSA in rabbit VIII and VIII. The antibodies were evaluated in terms of antibody response and affinity in a direct competitive ELISA.	117
Table 3.6	Comparison of mouse anti-mitragynine antibodies (1 st bleed – 3 rd bleed) raised against 16-COOH-MG-KLH in mouse I. The antibodies were evaluated in terms of antibody response and affinity in a direct competitive ELISA.	117

Table 3.7	Comparison of mouse anti-mitragynine antibodies (1 st bleed – 3 rd bleed) raised against MG-MAPs-16 in mouse II and mouse III. The antibodies were evaluated in terms of antibody response and affinity in a direct competitive ELISA.	118
Table 4.1	The plate layout of a checkerboard dilution for determination of the optimum enzyme-conjugate (HRP-PABA-MG) and antibody (from immunogen PABA-MG-BSA) dilutions.	134
Table 4.2	The plate layout of a checkerboard dilution for determination of the optimum enzyme-conjugate (HRP-MG) and antibody (from immunogen MG-cBSA) dilutions.	137
Table 4.3	Result of checkerboard titration (in absorbance value) for antibody from immunogen PABA-MG-BSA using enzyme-conjugate HRP-PABA-MG.	143
Table 4.4	Result of checkerboard titration (in B/B ₀ %) for antibody from immunogen PABA-MG-BSA using enzyme-conjugate HRP-PABA-MG.	144
Table 4.5	Dose response data of mitragynine to determine IC ₅₀ using antibody from immunogen PABA-MG-BSA in a direct competitive ELISA format.	146
Table 4.6	Comparison of HRP-MG and HRP-PABA-MG in ELISA performance using antibody from immunogen MG-cBSA.	148
Table 4.7	Result of checker board titration (in absorbance value) using different dilutions of antibodies and HRP-MG in dilution buffer.	149
Table 4.8	Summary of the percentage of cross-reactivity and the half maximal inhibitory concentration (IC ₅₀) for the study of structural similar drug to mitragynine.	151
Table 4.9	Reduction of matrix effects was determined by performing urine dilution (non-diluted urine, 5-fold and 10-fold diluted urine) in ELISA assay.	153
Table 4.10	Determination of limit of detection (LoD) and limit of quantification (LoQ) in the ELISA using 20 blank human urine samples.	162
Table 4.11	Table showing the percentage of recovery for the spiked QC samples at concentrations of 20 ng/mL (low), 50 ng/mL (medium), and 100 ng/mL (high).	163

Table 4.12	Intra-day assay precision was determined by performing six calibration curves within a day using the optimized ELISA assay.	164
Table 4.13	Inter-day assay reproducibility was determined by performing six calibration curves between days using the optimized ELISA assay.	165
Table 4.14	Analysis of urine samples collected from kratom users using the validated ELISA assay.	167
Table 5.1	Table showing sorbents for solid phase extraction (SPE) (Żwir-Ferenc & Biziuk, 2006).	173
Table 5.2	A summary of the LC-ESI-MS/MS parameters used for the development of the MRM method.	179
Table 5.3	Table showing the concentrations of working stock solution for mitragynine, 9-O-DM-MG, and 16-COOH-MG.	180
Table 5.4	Concentration of spiked samples of mitragynine, 9-O-DM-MG, and 16-COOH-MG for determination of limit of quantification (LoQ).	183
Table 5.5	A summary of the hydrolysis conditions used for the determination of the degree of hydrolysis of sulphate metabolites using β -glucuronidase/arylsulfatase enzyme from <i>Helix pomatia</i> .	185
Table 5.6	A summary of the HPLC conditions used to isolate metabolites (9-O-DM-G-MG, 9-O-DM-S-MG, 16-COOH-G-MG, 9-O-DM-16-COOH-S-MG, and 17-O-DM-DH-G-MG) from the positive human urine.	186
Table 5.7	A summary of product ions, fragmentor voltages and collision energy from the protonated molecule $[M+H]^+$ of mitragynine and nalorphine obtained from the Agilent MassHunter Optimizer – Automated MS Method Development Software.	188
Table 5.8	Mobile phase gradient timetable. B is refers to the organic phase (acetonitrile with 0.1% formic acid).	192
Table 5.9	Optimized MRM parameters for mitragynine, nalorphine, and kratom metabolites.	193
Table 5.10	Summary of intra-day and inter-day reproducibility on the percentage of accuracy for mitragynine, 9-O-DM-MG, and 16-COOH-MG.	203

Table 5.11	Summary of intra-day and inter-day reproducibility on the percentage recovery of mitragynine, 9-O-DM-MG, and 16-COOH-MG.	204
Table 5.12	Summary of percentage accuracy for the determination of limit of quantification (LoQ) of mitragynine, 9-O-DM-MG, and 16-COOH-MG.	205
Table 5.13	Quantification of positive human urine samples (n = 10) for mitragynine, 9-O-DM-MG, and 16-COOH-MG.	206
Table 5.14	Table showing the concentrations of conjugated glucuronides of 16-COOH-MG and 9-O-DM-MG found in the positive human urine.	208
Table 5.15	Summary of the efficiency of the sulphate conjugated metabolite (9-O-DM-S-MG) hydrolysis using enzyme β -glucuronidase/arylsulfatase at concentrations of 2,000, 4,000, and 8,000 units/mL.	209
Table 5.16	Summary of the percentage of cross-reactivity and the half maximal inhibitory concentration (IC ₅₀) for the study of kratom alkaloids.	211
Table 5.17	Comparison of ELISA result with LC-ESI-MS/MS (for mitragynine alone) data using 10 positive human urine samples.	212
Table 5.18	Comparison of ELISA result with LC-ESI-MS/MS (total concentration of mitragynine, 9-O-DM-MG, and 16-COOH-MG) data using 10 positive human urine samples.	213
Table B.1	Cross-reactivity data for structure similar and dissimilar molecules to mitragynine (in absorbance).	255
Table B.2	Cross-reactivity data for structure similar and dissimilar molecules to mitragynine (in B/B ₀ %).	256
Table B.3	Cross-reactivity data for kratom metabolites (in absorbance).	258
Table B.4	Cross-reactivity data for kratom metabolites (in B/B ₀ %).	259
Table B.5	Stability data of enzyme-conjugate (HRP-MG) in 4 types of stabilizers at 37°C.	261
Table B.6	Stability data of enzyme-conjugate (HRP-MG) in 4 types of stabilizers at 4°C.	262

Table B.7	Stability data of anti-mitragynine antibody in 4 types of stabilizers at 37°C.	263
Table B.8	Stability data of anti-mitragynine antibody in 4 types of stabilizers at 4°C.	264
Table B.9	Stability data of calibrators of mitragynine at 37°C. The percentage refers to B/B ₀ .	265
Table B.10	Stability data of calibrators of mitragynine at 4°C. The percentage refers to B/B ₀ .	266

LIST OF FIGURES

		Page
Figure 1.1	The diagrams showing the kratom powder (i), kratom flower (ii), kratom extract (iii), and kratom seeds (iv) (adapted from Mitragyna.com, 2012).	2
Figure 1.2	The diagrams showing the red vein kratom (i), and green vein kratom (ii) (adapted from Herbal Flame, 2015).	3
Figure 2.1	Molecular structure of mitragynine with possible sites for modification using various methods.	24
Figure 2.2	Reaction scheme for the synthesis of 4-aminobenzoic acid-mitragynine (PABA-MG) via diazotization.	30
Figure 2.3	The diagram showing the setup of Schlenk line apparatus (adapted from Millar, 2013).	33
Figure 2.4	Reaction scheme for the synthesis of 9-O-DM-MG via demethylation of mitragynine using ethanethiol.	33
Figure 2.5	Reaction scheme for demethylation of mitragynine using dimethyl sulfide.	34
Figure 2.6	Reaction scheme for demethylation of mitragynine using iodocyclohexane.	35
Figure 2.7	Reaction scheme for hydrolysis of mitragynine using trimethyltin hydroxide.	36
Figure 2.8	Reaction scheme for demethylation of mitragynine via acid hydrolysis.	36
Figure 2.9	Reaction scheme for demethylation of mitragynine via alkaline hydrolysis using sodium hydroxide.	37
Figure 2.10	Reaction scheme for the synthesis of 16-carboxymitragynine via alkaline hydrolysis using potassium hydroxide.	38
Figure 2.11	Reaction scheme for demethylation of mitragynine via alkaline hydrolysis using lithium hydroxide.	39

Figure 2.12	Reaction scheme for alkylation of mitragynine using ethyl-5-bromovalerate, followed by hydrolysis. Three possible products (i), (ii), and (iii) are expected to form after the reaction.	41
Figure 2.13	Reaction scheme for alkylation of mitragynine using 3-bromopropionic acid (cold condition).	42
Figure 2.14	Reaction scheme for alkylation of mitragynine using 3-bromopropionic acid (hot condition).	43
Figure 2.15	Reaction scheme for alkylation of mitragynine using 3-iodopropionic acid.	44
Figure 2.16	Reaction scheme for reduction of mitragynine using sodium borohydride.	45
Figure 2.17	Reaction scheme for reduction of mitragynine using lithium aluminium hydride.	45
Figure 2.18	Reaction scheme for oxidation of mitragynine using potassium permanganate.	46
Figure 2.19	Reaction scheme for the synthesis of MG-cBSA via Mannich reaction.	47
Figure 2.20	Molecular structure of 6-aminocaproic acid (6-ACA).	48
Figure 2.21	Reaction scheme for the synthesis of MG-BSA-6-ACA via Mannich reaction.	49
Figure 2.22	Molecular structure of bis-(3-aminopropyl)-amine (Bis-(3-APA)).	49
Figure 2.23	Reaction scheme for the synthesis of MG-BSA-bis-(3-APA) via Mannich reaction.	50
Figure 2.24	Reaction scheme for the synthesis of MG-KLH via Mannich reaction.	51
Figure 2.25	Reaction scheme for the synthesis of MG-MAPs-16 via Mannich reaction.	51
Figure 2.26	Reaction scheme for the synthesis of PABA-MG-BSA.	52
Figure 2.27	Reaction scheme for the synthesis of PABA-MG-cBSA.	53
Figure 2.28	Reaction scheme for the synthesis of PABA-MG-KLH.	53

Figure 2.29	Reaction scheme for the conjugation of 9-O-DM-MG to BDDE linker.	55
Figure 2.30	Reaction scheme for the synthesis of 9-O-DM-MG-BSA.	55
Figure 2.31	Reaction scheme for the synthesis of 9-O-DM-MG-KLH.	55
Figure 2.32	Reaction scheme for the synthesis of 16-COOH-MG-BSA via carbodiimide method.	56
Figure 2.33	Reaction scheme for the synthesis of 16-COOH-MG-KLH via carbodiimide method.	57
Figure 2.34	Reaction scheme for the synthesis of MG-BSA via photoactivation using Sulfo-NHS-SS-Diazirine (sulfo-SDAD).	58
Figure 2.35	Reaction scheme for the synthesis of HRP-MG via Mannich reaction.	59
Figure 2.36	Reaction scheme for the synthesis of HRP-PABA-MG via carbodiimide method.	60
Figure 2.37	Reaction scheme for the synthesis of HPR-9-O-DM-MG via homobifunctional linker (BDDE).	61
Figure 2.38	Reaction scheme for the synthesis of HRP-16-COOH-MG via carbodiimide method.	61
Figure 2.39	Scheme for the addition of standards of carrier proteins solution and samples (protein-hapten conjugates) in Nunc multiwell plate according to their respective concentrations and dilutions.	62
Figure 2.40	¹³ C NMR spectrum of 9-hydroxymitragynine in CDCl ₃ .	69
Figure 2.41	¹ H NMR spectrum of 9-hydroxymitragynine in CDCl ₃ .	70
Figure 2.42	¹ H – ¹³ C HMBC spectrum of 9-hydroxymitragynine in CDCl ₃ .	71
Figure 2.43	Reaction scheme for the PABA-MG linked to carrier proteins via carbodiimide method.	80
Figure 2.44	Molecular structure of dye Coomassie Brilliant Blue G-250.	83
Figure 2.45	The calibration curve of absorbance versus concentration of BSA was plotted to determine the synthesized PABA-MG-BSA concentration.	84

Figure 2.46	The calibration curve of absorbance versus concentration of cBSA was plotted to determine the synthesized PABA-MG-cBSA concentration.	84
Figure 2.47	The calibration curve of absorbance versus concentration of KLH was plotted to determine the synthesized PABA-MG-KLH concentration.	85
Figure 2.48	The calibration curve of absorbance versus concentration of cBSA was plotted to determine the synthesized MG-cBSA concentration.	85
Figure 2.49	The calibration curve of absorbance versus concentration of BSA-6-ACA was plotted to determine the synthesized MG-BSA-6-ACA concentration.	86
Figure 2.50	The calibration curve of absorbance versus concentration of BSA-Bis-(3-APA) was plotted to determine the synthesized MG-BSA-bis-(3-APA) concentration.	86
Figure 2.51	The calibration curve of absorbance versus concentration of KLH was plotted to determine the synthesized MG-KLH concentration.	87
Figure 2.52	The calibration curve of absorbance versus concentration of BSA was plotted to determine the synthesized 9-O-DM-MG-BSA concentration.	87
Figure 2.53	The calibration curve of absorbance versus concentration of KLH was plotted to determine the synthesized 9-O-DM-MG-KLH concentration.	88
Figure 2.54	The calibration curve of absorbance versus concentration of BSA was plotted to determine the synthesized 16-COOH-MG-BSA concentration.	88
Figure 2.55	The calibration curve of absorbance versus concentration of KLH was plotted to determine the synthesized 16-COOH-MG-KLH concentration.	89
Figure 2.56	Molecular structure of 2,4,6-trinitrobenzene sulfonic acid (TNBS).	90
Figure 2.57	Reaction scheme of 2,4,6-trinitrobenzene sulfonic acid (TNBS) with primary amine groups of amino acids to form yellow adducts.	90
Figure 2.58	Molecular structure of sinapinic acid (SA).	92

Figure 2.59	Molecular structure of α -cyano-4-hydroxycinnamic acid (CHCA).	92
Figure 3.1	The main structure of immunoglobulin (Ig) classes: IgG (i), IgE (ii), IgD (iii), IgA dimer (iv), and IgM pentamer (v).	98
Figure 3.2	The diagram illustrating the primary and secondary antibody response to an antigen over a period of time (Rogers, 2006).	102
Figure 3.3	The diagram illustrating the antigens was mixed by using two glass syringe attached to a 3-way stopcock (Muller, 2016).	107
Figure 4.1	The diagrams showing the steps involved in antigen-labelled competitive ELISA (i) and antibody-labelled competitive ELISA (ii).	124
Figure 4.2	The diagram showing the steps involved in the sandwich ELISA format.	126
Figure 4.3	The diagram showing the steps involved in the indirect ELISA format.	128
Figure 4.4	Reaction scheme for oxidation of 3,3',5,5'-tetramethylbenzidine (TMB) substrate to yield soluble blue product (adapted from GeneTex Inc, 2013).	129
Figure 4.5	Layout of 96-well microtiter plate for ELISA assay.	135
Figure 4.6	Dose response curve of mitragynine for antibody from immunogen PABA-MG-BSA was plotted to determine IC ₅₀ value.	146
Figure 4.7	A linear calibration curve of mitragynine with concentration range of 5 – 450 ng/mL using HRP-MG (1:3,000 dilution) and antibody from immunogen MG-cBSA (1:2,000 dilution) in dilution buffer.	150
Figure 4.8	The graphs showing the stability of enzyme-conjugate HRP-MG by storing at 37°C (i) and 4°C (ii) in four types of stabilizers (HRP Stabilzyme, HRP Stabilguard, HRP Select, and HRP F1H (in-house)).	155
Figure 4.9	The graphs showing the stability of antibody from immunogen MG-cBSA by storing at 37°C (i) and 4°C (ii) in four types of stabilizers (HRP Stabilzyme, HRP Stabilguard, HRP Select, and HRP F1H (in-house)).	157

Figure 4.10	The graphs showing the stability of calibrators of mitragynine by storing at 37°C (i) and 4°C (ii) in 10-fold diluted urine contain 0.01% sodium azide.	159
Figure 4.11	A linear calibration curve of mitragynine with concentration range of 2 – 200 ng/mL where the antibody (1:2,000 dilution) and enzyme-conjugate (1:4,000 dilution) in HRP Stabilzyme are used in the ELISA assay.	160
Figure 4.12	The graph showing the average of six calibration curves performed within a day using the optimized ELISA assay.	164
Figure 4.13	The graph showing the average of six calibration curves performed between days using the optimized ELISA assay.	166
Figure 5.1	A typical process of solid phase extraction (1. Conditioning. 2. Loading sample. 3. Washing. 4. Eluting.) (adapted from John Morris Scientific).	172
Figure 5.2	Molecular structure of nalorphine.	189
Figure 5.3	Calibration curves with peak area ratio plotted against the concentrations of mitragynine (i), 9-hydroxymitragynine (9-O-DM-MG)(ii), and 16-carboxymitragynine (16-COOH-MG)(iii).	196
Figure 5.4	The MRM chromatograms of mitragynine for determining matrix interference at its retention time of 6.482 min as marked by ↓. The data showed insignificant or no interference at the target analyte retention time.	198
Figure 5.5	The MRM chromatograms of 9-O-DM-MG for determining matrix interference at its retention time of 5.768 min as marked by ↓. The data showed insignificant or no interference at the target analyte retention time.	199
Figure 5.6	The MRM chromatograms of 16-COOH-MG for determining matrix interference at its retention time of 5.780 min as marked by ↓. The data showed insignificant or no interference at the target analyte retention time.	200
Figure 5.7	These are MRM chromatograms of nalorphine (internal standard) showing that there was no matrix interference at its retention time of 3.723 – 3.725 min.	201
Figure 5.8	Correlation curve between ELISA and LC-MS/MS (for mitragynine only).	213

Figure 5.9	Correlation curve between ELISA and LC-MS/MS (total concentration of mitragynine, 9-O-DM-MG, and 16-COOH-MG).	214
Figure A.1	Mass spectrum of carrier protein BSA.	237
Figure A.2	Mass spectrum of PABA-MG-BSA.	238
Figure A.3	Mass spectrum of carrier protein cBSA.	239
Figure A.4	Mass spectrum of PABA-MG-cBSA.	240
Figure A.5	Mass spectrum of carrier protein cBSA.	241
Figure A.6	Mass spectrum of MG-cBSA.	242
Figure A.7	Mass spectrum of carrier protein BSA-6-ACA.	243
Figure A.8	Mass spectrum of MG-BSA-6-ACA.	244
Figure A.9	Mass spectrum of carrier protein BSA-bis-(3-APA).	245
Figure A.10	Mass spectrum of MG-BSA-bis-(3-APA).	246
Figure A.11	Mass spectrum of MAPs-16.	247
Figure A.12	Mass spectrum of MG-MAPs-16.	248
Figure A.13	Mass spectrum of carrier protein BSA.	249
Figure A.14	Mass spectrum of 9-O-DM-MG-BSA.	250
Figure A.15	Mass spectrum of carrier protein BSA.	251
Figure A.16	Mass spectrum of 16-COOH-MG-BSA.	252
Figure A.17	Mass spectrum of Sulfo-SDAD-BSA.	253
Figure A.18	Mass spectrum of MG-BSA using Sulfo-SDAD.	254
Figure B.1	Cross-reactivity curve for structure similar and dissimilar molecules to mitragynine.	257
Figure B.2	Cross-reactivity curve for kratom metabolites.	260
Figure F.1	¹ H NMR spectrum of mitragynine dissolved in CDCl ₃ .	290
Figure F.2	FT-IR spectrum of mitragynine.	291
Figure F.3	Mass spectrum of mitragynine in ESI positive mode.	292

Figure F.4	Mass spectrum and chromatogram of 16-carboxymitragynine (16-COOH-MG).	293
Figure F.5	Ion chromatogram of 9-O-DM-S-MG.	294
Figure F.6	Ion chromatogram of 9-O-DM-G-MG and 16-COOH-G-MG.	294
Figure F.7	Ion chromatogram of 17-O-DM-DH-G-MG.	294

LIST OF ABBREVIATIONS

16-COOH-G-MG	16-carboxymitragynine glucuronide
16-COOH-MG	16-carboxymitragynine
17-COOH-DH-MG	17-carboxy-16,17-dihydropmitragynine
17-O-DM-DH-G-MG	17- <i>o</i> -demethyl-16,17-dihydropmitragynine glucuronide
17-O-DM-DH-MG	17- <i>o</i> -demethyl-16,17-dihydropmitragynine
6-ACA	6-aminocaproic acid
7-OH-MG	7 α -hydroxy-7H-mitragynine
9,17-O-BDM-DH-MG	9, 17- <i>o</i> -bis-demethyl-16,17-dihydropmitragynine
9,17-O-BDM-DH-S-MG	9,17- <i>o</i> -bis-demethyl-16,17-dihydropmitragynine sulphate
9-O-DM-16-COOH-MG	9- <i>o</i> -demethyl-16-carboxymitragynine
9-O-DM-16-COOH-S-MG	9- <i>o</i> -demethyl-16-carboxymitragynine sulphate
9-O-DM-G-MG	9- <i>o</i> -demethylmitragynine glucuronide
9-O-DM-MG	9- <i>o</i> -demethylmitragynine
9-O-DM-S-MG	9- <i>o</i> -demethylmitragynine sulphate
amu	Atomic mass unit
A. U.	Absorbance unit
AADK	National anti-drug agency of Malaysia
ACN	Acetonitrile
AlCl ₃	Aluminium chloride
AMP	Amphetamine
APC	Antigen presenting cells
BDDE	1,4-butanediol diglycidyl ether

Bis-(3-APA)	Bis-(3-aminopropyl)-amine
cBSA	Cationized-bovine serum albumin
CD4	Cluster of differentiation 4
CFA	Complete freund adjuvant
DCM	Dichloromethane
CHCA	α -cyano-4-hydroxycinnamic acid
COC	Cocaine
CV	Coefficient of variance
CYP2E1	Cytochrome P450, family 2, subfamily E, polypeptide 1
Da	Dalton
DMF	Dimethylformamide
DMS	Dimethyl sulfide
DMSO	Dimethyl sulfoxide
EDA.2HCl	Ethylenediamine dihydrochloride
EDC	1-ethyl-3-(3-dimethylaminopropyl)-carbodiimide hydrochloride
EIA	Enzyme immunoassay
ELISA	Enzyme-linked immunosorbent assay
ESI	Electrospray ionization
EtSH	Ethanethiol
GC-MS	Gas chromatography mass spectrometry
GC-MS/MS	Gas chromatography tandem mass spectrometry
HCl	Hydrochloric acid
HI	Hydrogen iodide
HMBC	Heteronuclear multiple bond correlation

HPLC-DAD	High performance liquid chromatography coupled to diode array detector
HPLC-UV	High performance liquid chromatography coupled to ultra violet detector
HRP	Horseradish peroxidase
HSA	Human serum albumin
IFA	Incomplete freund adjuvant
K ₂ CO ₃	Potassium carbonate
KLH	Keyhole limpet haemocyanin
KMnO ₄	Potassium permanganate
KOH	Potassium hydroxide
LC-MS/MS	Liquid chromatography tandem mass spectrometry
LiAlH ₄	Lithium aluminium hydride
LiOH.H ₂ O	Lithium hydroxide monohydrate
LLE	Liquid-liquid extraction
LoD	Limit of detection
LoQ	Limit of quantification
MALDI-TOF	Matrix assisted laser desorption/ionization-time of flight
MAP	Multiple antigenic peptide
MDMA	3,4-methylenedioxy-methamphetamine (Ecstasy)
MG	Mitragynine
MHC	Major histocompatibility complex
MOP	Morphine
MRM	Multiple reaction monitoring
MSE	<i>Mitragyna speciosa</i> alkaloid extract
MTD	Methadone

Na ₂ SO ₄	Sodium sulphate
NaBH ₄	Sodium borohydride
NaCl	Sodium chloride
NaH	Sodium hydride
NaHCO ₃	Sodium bicarbonate
NaNO ₂	Sodium nitrite
NaOH	Sodium hydroxide
NH ₄ Cl	Ammonium chloride
NHS	N-Hydroxysuccinimide
NMR	Nuclear magnetic resonance
PABA	Para-aminobenzoic acid
PAY	Paynantheine
PBS	Phosphate buffered saline
pI	Isoelectric point
QC	Quality control
R _f	Retention factor
RIA	Radioimmunoassay
RMP	Royal Malaysian police
RSP	Reserpine
S/N	Signal to noise ratio
SA	Sinapinic acid
SAM	Sheep-Anti-Mouse
SAR	Sheep-Anti-Rabbit
SAS	Saturated ammonium sulphate
SC	Speciociliatine

SCX	Strong cation exchange
SDS	Sodium dodecyl sulphate
SPE	Solid phase extraction
Sulfo-SDAD	Sulfo-NHS-SS-Diazirine
SUSDP	Standard for the uniform scheduling of drugs and poisons (Australia)
TFA	Trifluoroacetic acid
THG	Thyroglobulin
TLC	Thin layer chromatography
TMB	3,3',5,5'-tetramethylbenzidine
TMTOH	Trimethyltin hydroxide
TNBS	2,4,6-trinitrobenzene sulfonic acid

LIST OF SYMBOLS

%	Percentage
°C	Degree Celcius
μg/mL	Microgram/millilitre
μL	Microlitre
μm	Micrometre
cm	Centimetre
eV	Electron Volt
G	Gauge (measure size of needle)
g/moL	Gram/moles
IC ₅₀	Half maximal inhibitory concentration
M	Molar
mg/kg	Milligram/kilogram
mg/mL	Milligram/millilitre
mL/min	Millilitre/minute
N	Normality
ng/mL	Nanogram/millilitre
nm	Nano meter
pKa	Ionization constant
R ²	Coefficient of determination
β	<i>Beta</i>
V	Voltage
v/v	Volume/volume

PEMBANGUNAN IMUNOESEI UNTUK MITRAGININ

ABSTRAK

Ketum merupakan tumbuhan tropika yang digunakan dalam perubatan tradisional untuk mengurangkan kesakitan dan merawat cirit-birit. Walau bagaimanapun, di Malaysia, ketum seringkali disalahgunakan sebagai dadah rekreasi disebabkan kesan rangsangan sistem saraf pusat dan kekerapan penyalahgunaannya semakin meningkat semenjak 2005. Mitraginin (MG), substrat/bahan aktif ketum, telah dibuktikan boleh menyebabkan ketagihan. Oleh sebab itu, kini dibawah Akta Racun 1952, ketum adalah bahan kawalan di mana pemilikan ketum dianggap salah di sisi undang-undang. Justeru itu, ujian saringan air kencing diperlukan. Oleh yang demikian, objektif utama projek ini adalah untuk membangunkan suatu imunoesei untuk mengesan mitraginin dan metabolit-metabolitnya di dalam air kencing manusia. Untuk menghasilkan antibodi terhadap mitraginin, ia telah digandingkan kepada protein pembawa, albumin serum lembu yang dikationkan (cBSA) melalui tindak balas Mannich. Antigen yang disintesis ini disuntikkan ke dalam dua arnab untuk mendapatkan antibodi poliklonal terhadap mitraginin. Antibodi-antibodi dikumpulkan seminggu selepas imunasi kedua. Enzim konjugat mitraginin-HRP telah disintesis sebagai reagen pengesan melalui tindak balas Mannich. Kedua-dua antibodi dan enzim konjugat dioptimalkan dalam imunoesei demi pencirian antibodi mitraginin. Imunoesei menggunakan antibodi mitraginin dengan enzim konjugat mitraginin-HRP membawa nilai IC_{50} sebanyak 8.38 ng/mL. Kereaktifan-silang antibodi dengan 7 α -hydroxy-7H-mitragynine (82.65%), speciociliatine (63.20%), dan paynantheine (54.35%) menggunakan enzim konjugat mitraginin-HRP. Imunoesei yang

dibangkitkan menunjukkan had pengesanan bernilai 15.05 ng/mL untuk air kencing dan had kuantifikasi pada 27.23 ng/mL di mana sampel air kencing cuma dicairkan 10 kali ganda dengan larutan penampapan. Keputusan intra- dan inter-esei yang didapati adalah dalam lingkungan 1.50 – 8.05%. Suatu kaedah kromatografi cecair-ionisasi elektropray-spektrometri jisim (LC-ESI-MS/MS) telah dibangunkan dan disahkan untuk pengesanan mitraginin dan metabolit-metabolitnya di dalam air kencing manusia. Oleh yang demikian, imunoesei yang dibangkitkan ini diberi pengesanan dan keputusan yang diperolehi dikaitkan dengan data daripada LC-ESI-MS/MS. Sepuluh sampel air kencing positif manusia telah dianalisa dan dikuantifikasikan dengan imunoesei yang telah dibangkitkan dan keputusan ini dibandingkan dengan kaedah LC-ESI-MS/MS yang menunjukkan korelasi baik dengan bernilai $R^2 = 0.7426$. Data yang diperolehi daripada imunoesei ini menunjukkan jumlah kepekatan yang diperolehi daripada sampel-sampel air kencing positif ini adalah dalam lingkungan 6.62 – 81.51 $\mu\text{g/mL}$. Sampel-sampel ini menunjukkan kepekatan mitraginin pada 0.45 – 9.81 $\mu\text{g/mL}$, 9-O-DM-MG pada 5.52 – 24.23 $\mu\text{g/mL}$, dan 16-COOH-MG pada 4.01 – 14.85 $\mu\text{g/mL}$ apabila dianalisis dengan LC-ESI-MS/MS. Ini meliputi jumlah kepekatan dalam lingkungan 11.00 – 44.35 $\mu\text{g/mL}$. Kesimpulannya, suatu imunoesei telah berjaya dibangunkan dan disahkan untuk kegunaannya dalam pengesanan mitraginin dan metabolit-metabolitnya dalam air kencing manusia. Di samping itu, kaedah LC-ESI-MS/MS yang telah disahkan sesuai digunakan sebagai kaedah pengesanan.

DEVELOPMENT OF AN IMMUNOASSAY FOR MITRAGYNE

ABSTRACT

Kratom is a tropical plant used in traditional medicine for pain relief and to treat diarrhea. However, in Malaysia kratom is commonly misused as a recreational drug due to its central nervous system stimulatory effect and its frequency of abuse has been on the rise since 2005. Mitragynine (MG) an active ingredient in kratom has been proven to be addictive. Thus, possession of kratom is now illegal and controlled under the Poisons Act 1952. Therefore, a rapid screening urine test needs to be developed. For effective enforcement to monitor the kratom abuse, the main objective of this project was to develop an immunoassay for the detection of mitragynine residues and its metabolites in human urine. To raise anti-mitragynine antibodies, mitragynine was conjugated to the carrier protein, cationized-bovine serum albumin (cBSA) directly using the Mannich reaction. The synthesized antigen was injected into two rabbits to raise polyclonal antibodies against mitragynine. The antibodies were harvested a week post the (2nd) booster immunization. Horseradish peroxidase-mitragynine (HRP-MG) conjugate was synthesized via Mannich reaction and used as a tracer. These antibodies and enzyme-conjugate were optimized for antibody characterization. The antibody assay using HRP-MG produced an IC₅₀ of 8.38 ng/mL. The antibody cross-reacted with 7 α -hydroxy-7H-mitragynine (82.65%), speciociliatine (63.20%), and paynantheine (54.35%) using HRP-MG. The immunoassay developed showed a limit of detection (LoD) of 15.05 ng/mL (ppb) and a limit of quantification (LoQ) of 27.23 ng/mL (ppb) in urine whereby the urine samples were diluted 10 times with dilution buffer. The variation of intra-day and

inter-day assay results ranged from 1.50 – 8.05%. A liquid chromatography tandem mass spectrometry (LC-ESI-MS/MS) method was developed and validated for the detection of mitragynine and its metabolites in human urine. Therefore, the developed immunoassay was validated and its results correlated with the LC-ESI-MS/MS data. Ten positive human urine samples were screened and quantified using the developed immunoassay method and their results compared with that of the LC-ESI-MS/MS method showed good correlation of $R^2 = 0.7426$. Data collected from the immunoassay showed positive urine samples with total concentration ranging from 6.62 – 81.51 $\mu\text{g/mL}$ (ppm). These positive samples analysed with the LC-ESI-MS/MS showed 0.45 – 9.81 $\mu\text{g/mL}$ (ppm) of mitragynine, 5.52 – 24.23 $\mu\text{g/mL}$ (ppm) of 9-O-DM-MG, and 4.01 – 14.85 $\mu\text{g/mL}$ (ppm) of 16-COOH-MG thus, giving a total concentration range of 11.00 – 44.35 $\mu\text{g/mL}$ (ppm). Therefore, it was concluded that an immunoassay was successfully developed and validated for the detection of mitragynine and its metabolites in human urine. The validated LC-ESI-MS/MS method was suitable to be used as a confirmation method.

CHAPTER 1

INTRODUCTION

1.1 *Mitragyna speciosa*

Mitragyna speciosa (Figure 1.1) is a tropical plant native to many Southeast Asian countries, such as Thailand, Malaysia and Myanmar. It is a member of the Rubiaceae family and goes by local names such as ‘kratom’, ‘kakuam’, ‘ithang’, and ‘thom’ in Thailand; ‘mambog’ in the Philippines; and ‘biak-biak’ and ‘daun ketum’ in Malaysia (Houghton *et al.*, 1991). The Malaysian name ‘biak-biak’ aptly refers to the ability of this plant to grow wild on different terrain and especially in swampy areas. The kratom tree can grow beyond 15.2 meters in height and 4.6 meters in diameter.

Like most plants in nature, kratom also exhibits medicinal properties such as antihypertensive, anti-diabetic, improvement of blood circulation, analgesic, antipyretic, to counter fatigue, as well as in the treatment of cough and diarrhea (Kumarnsit *et al.*, 2006; Assanangkornchai *et al.*, 2007; and Utar *et al.*, 2011). Its uses also extended to being a stimulant at low doses, and as an opium substitute at high doses, and this has led to its use for weaning off heroin addiction. The leaves produce these narcotic-like effects when smoked, chewed, or drunk as a suspension (Matsumoto *et al.*, 1997).

Addiction is common among kratom users leading to prolonged sleep with heavy use. Chronic users of kratom experience insomnia, anorexia, weight loss, stomach distension, nausea, constipation, increased urination, sweating, darkening of the skin especially the cheeks, and dryness of the mouth (Kumarnsit *et al.*, 2006; and

Chittrakarn *et al.*, 2008). On the other hand, withdrawal symptoms bring about aggression, tearfulness, hostility, inability to work, and muscle pain (Chan *et al.*, 2005). According to Assanangkornchai *et al.* (2007), men recorded a higher rate of kratom consumption compared to women. The majority of them also showed a concurrent use of cannabis and amphetamine at some time.



Figure 1.1 The diagram showing the kratom powder (i), kratom flower (ii), kratom extract (iii), and kratom seeds (iv) (adapted from Mitragyna.com, 2012).

There are two types of kratom differentiated by the colour of the veins of the leaf, i.e. red veins (Figure 1.2i) and green veins (Figure 1.2ii). Both types of kratom have different effects and are known to be taken simultaneously for better results. The red vein kratom is believed to have stronger biological activities especially sedation at low doses (Chittrakarn *et al.*, 2008). It is often used for pain relief and detoxing therapies.

Conversely, green vein kratom with its stimulating and euphoric effect, is often utilized as an antidepressant (Kumarnsit *et al.*, 2007).



Figure 1.2 The diagram showing the red vein kratom (i), and green vein kratom (ii) (adapted from Herbal Flame, 2015).

The leaves are consumed either as ground powder or boiled in water. They exert their biological effects within 5 to 10 minutes of ingestion and the effects last for 1 to 1.5 hours depending on the amount consumed (Hassan *et al.*, 2013). Kratom is known to have a biphasic effect with initial exhilaration followed by sedation. Chittrakarn *et al.* (2008) have proved that it is more a central nervous system stimulant rather than a depressant. Kumarnsit *et al.* (2007) in his study revealed that kratom demonstrated antidepressant activity without spontaneous motor stimulation at doses of 100, 300 and 500 mg/kg. Moreover, the consumption of 300 mg/kg of aqueous extract in rats inhibits ethanol withdrawal-induced behaviours such as rearing, displacement and head weaving in a test of induction of ethanol withdrawal and treatment (Kumarnsit *et al.*, 2007). Chittrakarn *et al.* (2008) documented antidiarrheal effect on rat gastrointestinal tract using the kratom methanolic extract. Kratom leaves can also be used as an antimicrobial as well as antioxidant agent (Parthasarathy *et al.*, 2009). In summary, kratom possess anti-inflammatory, antinociceptive, anaesthetic, anti-

malaria, anti-diarrheal, anti-depressant, adrenergic, antioxidant, antimicrobial, and antitussive properties.

However, Saidin *et al.* (2008) showed dose-dependent cytotoxicity in several human cancer cell lines using the *Mitragyna speciosa* alkaloid extract (MSE). The data indicated that this cytotoxicity was enhanced in the presence of cytochrome enzyme, CYP2E1. A similar result was also observed with mitragynine, a major alkaloid constituent in kratom leaves.

1.2 Chemical constituents of *Mitragyna speciosa*

More than 40 alkaloids have been isolated from kratom. Alkaloids are nitrogenous compounds that exert a bitter taste. Most alkaloids are optically active and some of them exhibit curative properties (Ikan, 2013).

The two most abundant types of alkaloids are the indoles (mitragynine, paynantheine and speciogynine) and oxyindoles (mitraphylline and speciofoline). Mitragynine is the major alkaloid contributing 12 – 66.2% of the total alkaloid extract (Takayama, 2004). Paynantheine (8.6%) with a molecular formulae of $C_{23}H_{28}N_2O_4$ and a molecular weight of 397.0 g/mol, has the same configuration as speciogynine at C20 bearing a vinyl group instead of an ethyl group. Speciogynine (6.6%) is the third most abundant alkaloid present in kratom. It is a diastereomer of mitragynine which differs in the configuration at stereocenter C20. Both paynantheine and speciogynine act as a smooth muscle relaxant. Other smooth muscles relaxants also include speciociliatine, 7 α -hydroxy-7H-mitragynine and mitraciliatine. Speciociliatine (0.8%), a C3 stereoisomer of mitragynine, is a weak opioid agonist. Its potency at the opioid

receptor is 13-fold less than mitragynine. Moreover, speciociliatine, speciogynine, and paynantheine were shown to inhibit the naloxone-insensitive twitch contraction in rats (Takayama, 2004).

The geographical location of kratom results in variation of alkaloid constituents in its leaves (Takayama, 2004). It was reported that the major alkaloid, mitragynine, isolated from kratom growing in Thailand constitutes 66.2% of total chemical constituent compared to 12% with the Malaysian variant. Five identical alkaloids obtained from both the Thailand and Malaysia variants include mitragynine, speciogynine, speciociliatine, paynantheine, and 7 α -hydroxy-7H-mitragynine. In 1975, Hemingway *et al.* discovered three new speciofoline isomers. They were mitrafoline, isomitrafoline, and isospeciofoline. Mitrafoline, a non-phenolic 9-hydroxyrhynchophylline-type alkaloid, has identical chemical behaviour as rotundifoline. However, dissimilarity in a number of minor alkaloids found in the Malaysia variant differentiates it from the Thailand variant.

Houghton *et al.* (1991) showed that mitragynaline and corynantheidaline are the major alkaloids in very young leaves of kratom in Malaysia. But, mitragynaline is then found to be in minute quantities as the leaves mature. Other compounds like mitragynalic acid and corynantheidalinic acid remain as minor compounds in the leaves. Houghton and Said (1986) also isolated a new yellow coloured alkaloid 3-dehydromitragynine that gave rise to yellow colouration skin for kratom users. In 2000, Takayama *et al.* discovered a new corynanthe-type indole alkaloid named as (-)-9-methoxymitralactonine.

Another compound, 9-hydroxycorynantheidine, bears a hydroxyl group at C9 instead of a methoxy group. Matsumoto *et al.* (2006) verified that 9-hydroxycorynantheidine was a partial agonist of opioid receptors. The transformation from methoxy group (mitragynine) to hydroxy group (9-hydroxycorynantheidine) or to hydrogen (corynantheidine) at C9 drastically shifted it from a full agonist to an antagonist of opioid receptors (Takayama, 2004). The 9-hydroxycorynantheidine inhibited the electrically-induced twitch contraction with a maximum inhibition of 50%, which is lower than mitragynine.

Corynantheidine does not show any opioid agonist properties. Its antagonistic effect is concentration dependent. It inhibits the effect of morphine via functional antagonism of opioid receptors. Mitralactonal has a 9-methoxyindole nucleus. It shows long wavelength absorption at UV 496 nm indicating a high degree of unsaturation in the molecule (Takayama, 2004). All these unique alkaloids found in kratom (Table 1.1) have attracted a lot of researchers to study the chemical and pharmacological potentials of this plant such as mitragynine and 7 α -hydroxy-7H-mitragynine.

Table 1.1 Table showing the alkaloids found in *Mitragyna speciosa*.

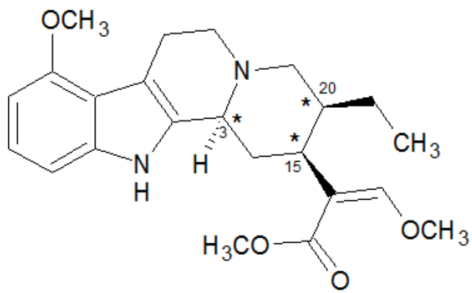
Alkaloid	Structure
Mitragynine (3S, 15S, 20S)	

Table 1.1 Continued.

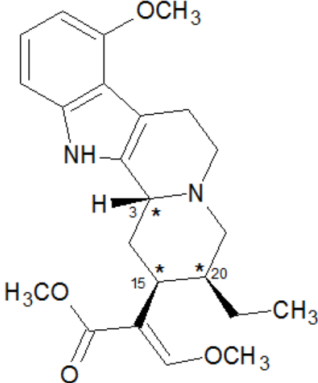
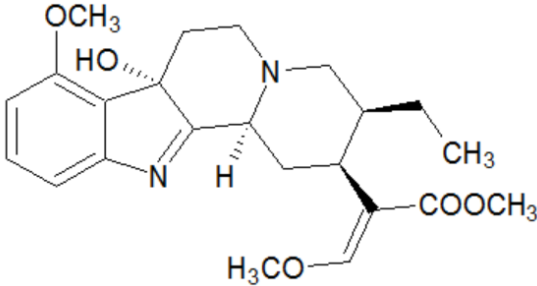
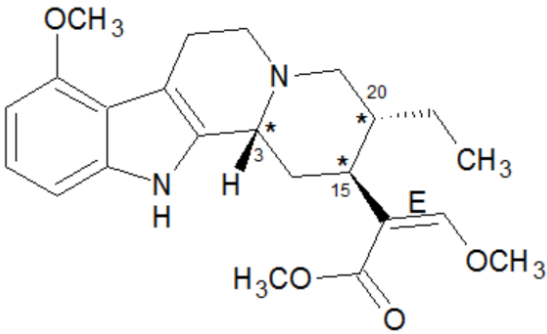
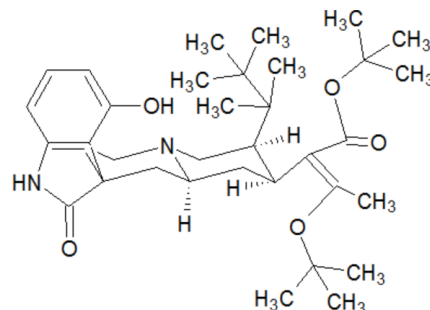
Alkaloid	Structure
Speciociliatine (3R, 15S, 20S)	 <p>The structure of Speciociliatine is a complex pentacyclic alkaloid. It features a benzene ring fused to an indole-like ring system, which is further fused to a piperidine ring. A third ring is a six-membered ring containing a nitrogen atom, fused to the piperidine ring. The structure is substituted with a methoxy group (OCH₃) on the benzene ring, a hydrogen atom (H) at position 3, a methoxy group (H₃CO) and a methyl group (CH₃) at position 15, and a methyl group (CH₃) and a methoxy group (OCH₃) at position 20. The stereochemistry is indicated by wedged and dashed bonds.</p>
7 α -hydroxy-7H-mitragynine	 <p>The structure of 7α-hydroxy-7H-mitragynine is a complex pentacyclic alkaloid. It features a benzene ring fused to an indole-like ring system, which is further fused to a piperidine ring. A third ring is a six-membered ring containing a nitrogen atom, fused to the piperidine ring. The structure is substituted with a methoxy group (OCH₃) and a hydroxyl group (HO) at position 7, a hydrogen atom (H) at position 7, a methyl group (CH₃) and a methoxy group (COOCH₃) at position 15, and a methyl group (CH₃) and a methoxy group (H₃CO) at position 20. The stereochemistry is indicated by wedged and dashed bonds.</p>
Mitraciliatine (3R, 15S, 20R)	 <p>The structure of Mitraciliatine is a complex pentacyclic alkaloid. It features a benzene ring fused to an indole-like ring system, which is further fused to a piperidine ring. A third ring is a six-membered ring containing a nitrogen atom, fused to the piperidine ring. The structure is substituted with a methoxy group (OCH₃) on the benzene ring, a hydrogen atom (H) at position 3, a methyl group (CH₃) and a methoxy group (H₃CO) at position 15, and a methyl group (CH₃) and a methoxy group (OCH₃) at position 20. The stereochemistry is indicated by wedged and dashed bonds.</p>

Table 1.1 Continued.

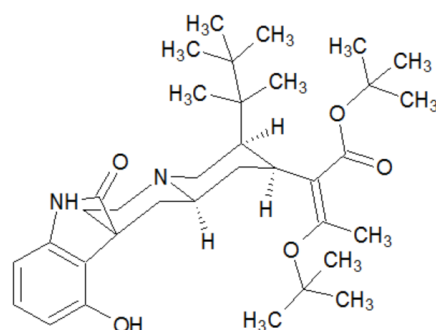
Alkaloid

Structure

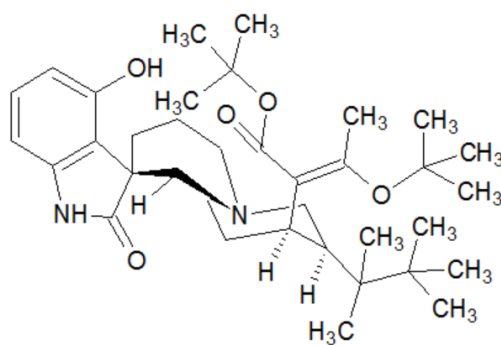
Mitrafoline



Isomitrafoline



Isospeciofoline



Mitragynaline

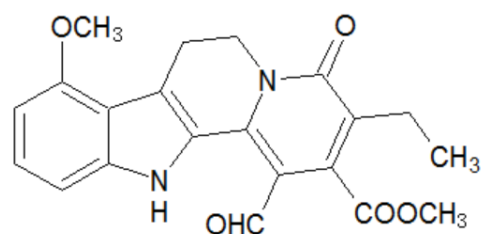


Table 1.1 Continued.

Alkaloid	Structure
Corynantheidaline	
Mitragynalic acid	
Corynantheidalinic acid	
(-)-9-methoxymitralactonine	
3-dehydromitragynine	

Table 1.1 Continued.

Alkaloid	Structure
Corynantheidine	
Mitrallactonal	
9-hydroxycorynantheidine	

1.2.1 Mitragynine

Mitragynine is the major alkaloid found in kratom. It was first isolated in 1921 and its structure fully elucidated in 1964. It has a molecular formula of $C_{23}H_{30}N_2O_4$ with a molecular weight of 398.50 g/mol. Its melting and boiling points range from 102 – 106°C and 230 – 240°C respectively. It is soluble in chloroform, alcohol, acetic acid, acetone and diethyl ether. It has an UV absorbance at 254 nm (Chee *et al.*, 2008). Chemically, it is named 9-methoxycorynantheidine due to the presence of a methoxy group at position C9. Compared to the general corynanthe-type indole alkaloids, it is

structurally characteristic of the Mitragyna alkaloid. The methoxy group at C9 is the key for pharmacophore binding to opioid receptors which controls the intrinsic activities on opioid receptors and elicits analgesic activity (Takayama *et al.*, 2002). It has an indole structure similar to reserpine, yohimbine, uncaria alkaloid, and other tryptamine compounds.

Mitragynine exhibits an uncommonly strong analgesic effect (Thongpradichote *et al.*, 1998). It is mediated by the μ - and δ - opioid receptors (Takayama *et al.*, 1995). Matsumoto *et al.* (1997) reported that mitragynine appeared to be a psychoactive drug. It produced analgesic and antitussive actions comparable to codeine without causing emesis or dyspnoea. Due to its structural similarity to codeine and morphine, comparison studies were conducted by Watanabe *et al.* (1997) on the analgesic effect of mitragynine on electrically stimulated contractions in the guinea-pig ileum. The results showed that analgesic activity by mitragynine was 6-fold less potent than morphine. Mitragynine itself can induce antinociceptive activity by acting in the brain and partially in the supraspinal opioid systems (Matsumoto *et al.*, 1996). Nevertheless, its analgesic qualities were further enhanced when it was used in combination with morphine and effectively impaired the development of substance tolerance. Furthermore, it also reduced liver toxicity as a result of chronic administration of morphine (Fakurazi *et al.*, 2013).

This is in accordance to the claim that kratom consumption results in anorexia and weight loss due to the inhibitory effect on gastric acid secretion via opioid receptors. Kumarnsit *et al.* (2006) showed that mitragynine administration resulted in decreased

weight gain in rats as well as indirectly lowered blood glucose level because of reduced food and water intake.

1.2.2 7 α -Hydroxy-7H-mitragynine

7 α -Hydroxy-7H-mitragynine is a terpenoid indole alkaloid with a molecular formula of C₂₃H₃₀N₂O₅ and a molecular mass of 414.50 g/mol. It accounts for 2% of the total alkaloid extract. Although it is present in minute amount in the plant, this novel opioid agonist is not only 13-fold more potent than morphine with less adverse effects (Matsumoto *et al.*, 2004), but it is also 46-fold more potent as an analgesic compared to mitragynine. Therefore, 7 α -hydroxy-7H-mitragynine is believed to be the most pharmacologically active alkaloid from *Mitragyna speciosa*.

7 α -Hydroxy-7H-mitragynine is structurally different from other opioid agonist and it exerts analgesia and euphoria in small doses. On the other hand, high doses bring about sedation. The hydroxyl group at position C7 enhances pharmacophore binding to μ -opioid receptors resulting in better oral absorption compared to morphine (Takayama *et al.*, 2002; Matsumoto *et al.*, 2004). Thus, 7 α -hydroxy-7H-mitragynine is a potential candidate for pain management and as an opiate substitute. However, it is most effective when used together with other alkaloids in the leaves.

1.3 Abuse of kratom

Drugs or substance abuse can be defined as drugs or substances consumption without approval by medical professionals. Individuals taking drugs for nonmedical purposes are not a new phenomenon. Drug abuse leads to social problems such as crime, unemployment, and violence. The National Anti-Drug Agency of Malaysia (AADK)

documented a total of 300,241 drug users from 1998 to 2006. That was approximately 1.1% of the Malaysian population (Vicknasingam & Mazlan, 2008). On 11 June 2012, the New Straits Times reported that young people aged between 18 and 39 tops the drug abuse list. Although kratom is not categorised as a drug, it is utilized in the same context as recreational drugs, i.e. heroin, methamphetamine, cannabis, ketamine, and ecstasy (MDMA).

The rampant abuse of kratom in Thailand and Malaysia, has forced both governments to raise awareness towards kratom (Houghton and Said, 1986) where it is claimed to cause addiction. Due to its opium-like effects, possession and ingestion of kratom are deemed illegal in both countries (Houghton *et al.*, 1991). Although Thailand has banned the usage of kratom since 1943, its use is still rampant as this plant is native to the country. Its use is also considered illegal in Australia, Myanmar, Vietnam and Denmark. Thus in 2004, mitragynine and kratom have been placed in schedule 9 of the Australian National Drugs and Poisons Schedule. Nevertheless, this plant remained uncontrolled in other countries like the United States of America and most countries in Europe (Chittrakarn *et al.*, 2008).

In 2006, many psychotropic herbal products adulterated with synthetic cannabinoids were found to be marketed worldwide rampantly especially through the internet. Their appearance in Japan since 2008 prompted Kikura-Hanajiri *et al.* (2011) to study and evaluate them. His survey findings revealed that mitragynine was detected in products at 1.2 – 6.3% and 7 α -hydroxy-7H-mitragynine ranging from 0.01 – 0.04%. Thus, kratom abuse became a foremost issue for concern.

Similar issues were seen in a survey on the prevalence of psychoactive drug usage among drivers in Thailand (Ingsathit *et al.*, 2009). Studies showed the use of mitragynine was increasingly popular and reportedly as one of the most common illicit drugs besides cannabis. In addition, a case report that indicated massive overdose of kratom could cause intrahepatic cholestasis (Kapp *et al.*, 2011). With its ability to produce euphoric effect, relaxation and pain relief similar to that of opium, these medicinal properties are due to be abused. Moreover, this plant is indigenous to Southeast Asian countries and is cheap to acquire. Consequently, this plant is illegal in these countries:

- Australia (placed in schedule 9 of the Australian SUSDP)
- Denmark
- Malaysia (mitragynine was listed in the First Schedule and Third Schedule (psychotropic substances) of the Poisons Act 1952 of January 2003 and kratom was deemed illegal without a government license since August 2006)
- Myanmar (under section 30(b) of the Narcotic Drugs and Psychotropic Substances Law)
- Thailand (classified as narcotic level 5)
- Vietnam

In other countries such as US, UK, and Germany, kratom usage is still not regulated. In Malaysia, there has been a growing trend among drug addicts who ingest kratom leaves to get high when they are unable to acquire their regular supply of cannabis or heroin. This kratom abuse has caused considerable concern among the public and law enforcement authorities. Its popularity is principally due to its wide availability and

low price compared to other illicit drugs. As mitragynine was found to be the major alkaloid of kratom, thus it was listed in the First Schedule and Third Schedule (psychotropic substances) of the Poisons Act 1952 of January 2003. Under the Act, planting the kratom tree is not an offense. However, individuals in possession or selling kratom leaves or drinks would be fined a maximum of RM10,000 or served four years jail or both (Chan *et al.*, 2005).

Lately, more stringent enforcement and regulation on kratom abuse was implemented. According to Malaysian country report, the government is in the final process of scheduling kratom under the Dangerous Drug Act 1952 to strengthen control of kratom by making its cultivation and trafficking illegal. Under the Dangerous Drug Act 1952, it provides mandatory death sentence for drug trafficking offenders (National Anti-Drugs Agency, Jun 2015).

1.4 Problem statement

Although kratom toxicity was insignificant and was a potential candidate as an alternative to methadone (Lago, 2013), this plant was still abused. This ultimately led to addiction. The increase of kratom abuse in Malaysia since 2005 caused many problems for the community such as crimes, neglect of family, poor work performance and also loss of consciousness. Extensive use of kratom results in prolonged sleep. The withdrawal symptoms include hostility, aggression, tearfulness, muscle pain and inability to work.

Hence, it is essential to not only control misuse of kratom but also to detect and monitor the users. Up till now, many chromatographic methods have been published to detect

mitragynine and other related alkaloids qualitatively and/or quantitatively. Although chromatographic methods using liquid chromatography (de Moraes *et al.*, 2009; Kikura-Hanajiri *et al.*, 2009; Lu *et al.*, 2009; Vuppala *et al.*, 2011; Le *et al.*, 2012; Parthasarathy *et al.*, 2013) or gas chromatography (Kaewklum *et al.*, 2005) are able to detect and confirm the presence of drugs quantitatively, however, the application of these methods are restricted by high analysis cost, and skilled/trained personnel are required. Hence, there is a need for the development of an immunoassay which is cheap, convenient and easy, rapid to use in screening for the presence of mitragynine (the major active alkaloid for kratom) in biological samples. It only requires a small amount of sample for analysis, no sample preparation is required, and simultaneous analyses of a large number of samples.

The contribution of this research work includes the reduction of kratom abuse by effective detection of users and minimization of social problems contributed by drug abusers through the development of a locally made ELISA test kit which is currently unavailable.

1.5 Objectives of study

The scope of this project encompasses the development of an immunoassay for the detection of mitragynine and its metabolites to monitor the kratom abusers. Therefore, the objectives of this research involve:

- To modify mitragynine for the use as a specific immunogen.
- To raise polyclonal antibodies towards mitragynine using the synthesized hapten.
- To synthesize mitragynine enzyme-conjugates for the use as a tracer in enzyme immunoassay.
- To optimize an enzyme immunoassay for the rapid screening of mitragynine and its metabolites.
- To characterize the polyclonal antibodies raised.
- To develop a validated liquid chromatography-tandem mass spectrometry (LC-ESI-MS/MS) method for the validation of the developed immunoassay and confirmation of mitragynine and its metabolites.

CHAPTER 2

HAPTEN MODIFICATION AND CONJUGATION

2.1 Introduction

The synthesis of a suitable hapten is critical in antibody production. It determines the affinity and the specificity of antibodies produced against the drug. Therefore, this chapter discusses the designations of the hapten mitragynine and its modifications as the first step to make antigen(s) for raising antibodies. Hapten refers to a small molecule e.g. a drug molecule which is too small to be immunogenic. Immunogenic molecules are huge molecules that are injected into animals to elicit an immune response. All immunogens are antigens but not all antigens are immunogens. Antigens are macromolecules which contain antigenic sites and are able to bind with antibodies in the immune system. Immunogenic compounds are foreign to the host system, have a high molecular weight and chemical complexity (Coico & Sunshine, 2009).

Molecules with a molecular weight of less than 5,000 Daltons (Da) are not considered an effective immunogen as they are unable to induce an immune response and produce hapten-specific antibodies (Crowther, 1995). This can be solved by coupling small molecule haptens to a large carrier protein which is able to stimulate the host immune response. Proteins are commonly used as carrier molecules due to their solubility and abundance of functional groups for conjugation. These carrier proteins can be keyhole limpet haemocyanin (KLH), bovine serum albumin (BSA), human serum albumin (HSA), thyroglobulin (THG), gamma globulins, fibrinogen, ovalbumin, synthetic polypeptides poly-L-lysine, and polyglutamic acid. The hapten-carrier conjugate can

be injected in any experimental animal except the animal of origin of the carrier protein itself.

Bovine serum albumin (BSA) is one of the most common protein used as it is cheap, physically and chemically stable, easily available, has good solubility, possesses numerous lysine residues and amino groups (Dewen *et al.*, 2007). Its molecular weight is 67,000 Da and possesses 59 lysine ϵ -amine groups (only 30 – 35 of lysine ϵ -amine groups are available for conjugation), 1 free cysteine sulfhydryl (with an additional 17 disulfides buried within its three-dimensional structure), 19 tyrosine phenolate residues, and 17 histidine imidazole groups. The presence of abundant carboxylate groups in BSA contributes to a net negative charge with pI value of 5.1. Modification of any carrier protein with hydrophobic haptens may result in precipitation due to the decrease of hydrophilicity. Therefore, the level of carrier protein modification in the conjugation reaction should not be too extensive in order to minimize precipitation (Hermanson, 2008).

Cationized-BSA (cBSA) is synthesized through the modification of the carboxylate groups of BSA using ethylenediamine. After modification of BSA, the negative charges contributed by the native carboxylates are masked and the positive charges from the amines are created. Thus, increasing its pI value (pI > 11.0) when compared to the native BSA. The higher pI value contributes to better immunogenicity whereby its rate of binding to APC is accelerated and consequently produce a quicker immune response (Hermanson, 2008).

Keyhole limpet haemocyanin (KLH) contains plenty of functional groups for conjugation purposes. Its molecular weight is more than 1,000,000 Da with more than 2,000 amines from lysine residues, over 700 sulfhydryls from cysteine groups, and more than 1,900 tyrosines. It is a multi-subunit protein which contains chelated copper of non-heme origin. Native KLH is stable and soluble in buffers containing at least 0.9 M sodium chloride (NaCl). Precipitation and denaturation happen at a concentration less than 0.6 M of NaCl. As a result, a high salt condition should be employed when multi-subunit KLH is used for conjugation. This is to maintain the solubility of the hapten-carrier complex. KLH should not be frozen due to freeze-thaw effect as it may cause denaturation. KLH is completely soluble in 50% DMSO and becomes cloudy at 60%. It precipitates at 67% of DMSO (Hermanson, 2008).

Ovalbumin has a molecular weight of 43,000 Da. It is a phosphoprotein that contains N-glycosylation sites with 386 amino acids. It has 20 lysine residues, 14 aspartic acids, and 33 glutamic acid groups with a pI value of 4.63. Solubility for ovalbumin in DMSO is up to 70%, become cloudy at 75% and precipitates at 80% (Hermanson, 2008).

Thyroglobulin (THG) is a protein stored in the thyroid gland. It has a molecular weight of 660,000 Da with a pI value of 4.7. Usually, THG and ovalbumin are used as non-relevant carriers in ELISA tests that measure antibody response. It is seldom used as carrier in the preparation of immunogens (Hermanson, 2008).

To modify a hapten, some factors need to be taken into consideration. First is the structural point of attachment for the hapten to a carrier protein. According to

Landsteiner's Principle, antibody specificity is directed primarily at the part of the hapten where it is furthest removed from the functional group that is used to couple to a carrier protein. This site of attachment provides steric hindrance by the carrier protein that prevents specific recognition of the hapten. Moreover, it is pendent for the hapten design to be attached to a carrier protein at a site remote from the chemical or metabolic change (Law, 1996).

The second consideration is the functionalization of the hapten. In order to covalently attach the hapten to a carrier protein, a suitable functional group must be present in hapten to react with complementary functional group on the carrier protein. The functional groups can be amino, carboxylic, aldehydes, ketones, thiol, and hydroxyl groups. A hapten without the necessary reactive functional groups need to be modified by introducing a reactive functional group into the structure prior to conjugation to the carrier protein. However, the final chemical structure and stereochemistry should be identical with the original hapten (Dewen *et al.*, 2007) to ensure greater antibody specificity.

The length of the spacer arm between hapten and carrier protein is important also to reduce the steric hindrance effect and allow the hapten to be more easily recognized by the circulating lymphocytes (Law, 1996). Long spacers cause the overlapping of hapten while short spacers may cause the carrier protein to obstruct the hapten and hence produce antibodies with a lack of specificity. According to Bermudez (1975), four to six carbon atoms of spacer groups are optimal for antigen-antibody interaction and to increase immunogenicity. Additionally, the spacer should be non-polar to avoid changes to the distribution of electric density of the hapten. Impurities as a result of

hapten synthesis not only reduce assay specificity but are also dangerous to the host animals as well. Hence, care must be taken to ensure good hapten quality and purity prior to immunization.

Selection of carriers is of utmost importance as different carrier protein induce different immune responses and affect antibody quality and quantity. This is because the secondary response is determined by the immunogenicity of the carrier proteins. Furthermore, the ratio of hapten per molecule of carrier protein has to be taken into consideration (Law, 1996) to prevent improper hapten designs that produce low quality antibodies.

In this research, mitragynine with a molecular mass of 398.5 g/mol is small and not sufficient to induce an immune response on its own. Hence, it must be conjugated to a carrier protein before being introduced into experimental animals. Besides, mitragynine does not have any suitable functional group for conjugation. Thus, introduction of relevant functional groups on mitragynine is needed such as carboxylic acid (-COOH), amino (-NH₂), hydroxyl (-OH), sulfhydryl group (-SH), aldehyde (-COH), and ketone (-C=O) groups that are suitable for coupling to a carrier protein. The possible sites for modification on mitragynine are shown in Figure 2.1.

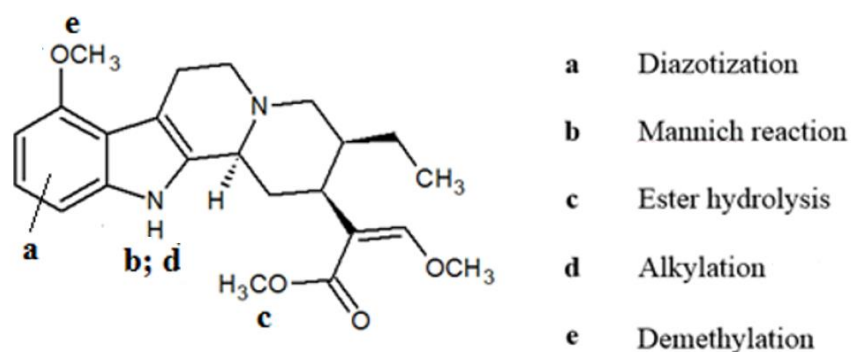


Figure 2.1 Molecular structure of mitragynine with possible sites for modification using various methods.

2.2 Aim of study

The main objective of this chapter is to design and modify the hapten mitragynine by introducing reactive functional groups and conjugating it to a carrier protein. Modification of carrier proteins is also performed in order to enable better conjugation and enhance the binding ratios. Subsequently, the concentrations and coupling ratios of successfully synthesized antigens are determined. Moreover, enzyme conjugates are also synthesized and used as a detection reagent in an enzyme-linked immunosorbent assay (ELISA).

2.3 Materials and instrumentation

Chemicals	Company/ Source
1,2-Dichloroethane	Sigma Aldrich Corporation, USA.
1,4-Butanediol diglycidyl ether $\geq 95\%$	Sigma Aldrich Corporation, USA.
1-Ethyl-3-(3-dimethylaminopropyl)-carbodiimide hydrochloride	Sigma Aldrich Corporation, USA.